Journal of Sustainable Metallurgy (2018) 4:233–250
https://doi.org/10.1007/s40831-018-0159-3

INNOVATIONS IN WEEE RECYCLING

Metallurgical Effects of Introducing Powdered WEEE to a Molten Slag Bath

Nikolaus Borowski[1] · Anna Trentmann[1] · Frederic Brinkmann[1] · Matthias Stürtz[1] · Bernd Friedrich[1]

Published online: 31 January 2018

Abstract
Powders and dusts from e-waste recycling processes are a valuable source for different metals like copper or precious metals such as silver and gold. Hence, the recycling of this fine fraction is of great interest. In addition to these precious metals, large amounts of organic, ceramic, and oxidic elements emerge, which have a tremendous influence on slag properties and the entire melting process. In order to recycle the valuable metals and use the energy of the material accompanying the organic constituents, the IME Institute of RWTH Aachen University is conducting research on the metallurgical effects of these fractions when introduced into a molten slag bath and developing solutions to recycle the component metals. Within this research, the influences on the slag phase are simulated using the thermochemical software FactSage™, and the material-specific oxygen amount required to combust the organic constituents is calculated. The results are tested and optimized in preliminary laboratory-scale experiments and later scaled up to technical size. The experimental results show a possible reduction in the slag phase's liquidus temperature by adding different additives and the feasibility of autothermal melting of fine fractions with good metal recovery rates and low metal distribution to the mineral phase.

Keywords WEEE-recycling · Powder · Autotherm · Slag properties · Injection · Pellet

General Background

In this world that is increasingly connected, which relies on electronic equipment and automation, electronics are playing a greater role in everyday technological products. The amount of e-waste that is generated all over the world is increasing annually along with growing production rates and global population growth [1]. Consequently, waste treatment and its recycling are of great interest. Over the last two decades, mechanical separation and conditioning followed by pyrometallurgical processes were the main focus for recycling electronic wastes [2]. These pyrometallurgical methods were promoted for the recycling of e-wastes because they are able to handle all kinds of electronic wastes with only limited amounts of previous separation, sorting, and conditioning processes. With the growing recycling rates of e-wastes, the amounts of waste fractions, which occur during the mechanical treatment of electronic scraps, are also steadily increasing. Because of their high metal content—especially in terms of precious metals—e-waste powders and dusts have become a more and more interesting source. However, the input amounts of electronic scrap powders and dusts into the existing recycling routes, e.g., pyrometallurgical copper recycling are limited because of the associated impurities (organics, ceramics, and oxides) which lead to alterations of the main melting process as well as challenges associated with the small particle size [3].

In other industries, especially in the steel making industry, iron powders and metallurgical dusts are already a well-known recyclable waste stream. Here, the two main furnace-feeding concepts for fine products are, on the one hand pelletizing processes where powders are agglomerated and sintered to mostly spherical pellets, and on the other hand, injection processes where dusts and powders for melt treatment are pneumatically transported and

The contributing editor for this article was Hiromichi Takebe.

✉ Nikolaus Borowski
nborowski@ime-aachen.de

[1] IME-Institute of Process Metallurgy and Metal Recycling, RWTH Aachen University, Intzestraße 3, 52056 Aachen, Germany

injected by lances into the melt [4]. Recycling can be carried out with self-reducing pellets made of waste streams like dusts and sludges with embedded carbon [5]. Investigations about their reduction behaviors in relation to time and temperature have been conducted by Kowitwarangkul et al. [6]. Detailed experimental results for the reduction kinetics are provided by Nascimiento et al. [7].

In steel plants, dusts and powders are often, when not pelletized or sintered, injected into the furnace. Many studies have been carried out to investigate the usage and optimization of injection technologies for fine powders. In this paper, however, only those exemplary studies with a similarity to the project at hand will be mentioned. The studies by Lahiri et al. and Liukkonen et al. about carbon injection into the slags of electric steel production to produce a foamy slag describe the causes and phenomenon of foamy slags as well as their control [8, 9]. The general advantages of foamy slags in metal production processes such as higher metal yield and increased reaction rates of carbon are described and discussed by Merz et al. [10]. A "zero waste metallurgy" through the recycling of zinc-containing baghouse dusts and oily mill scales is also described by Shaw et al., where dusts and mill scales were mixed with carbon as reducing agents and injected into the melting zone of an EAF-furnace. It was demonstrated how the wastes can be significantly reduced and recycled in an economic and efficient manner [11]. Further information about furnace dust recycling in different processes can be obtained from [12, 13].

The general concept behind this research was to adopt the basics of both methods for the recycling of fine fractions from E-waste conditioning and melting processes.

State of the Art of WEEE Processing

Nowadays, research and industrial processes are applied to recover the valuable materials from e-wastes, with most efforts focusing on the recovery of metal fractions due to their high economic value [14]. In general, metals found in electronic waste can be classified into five main groups: base metals (BMs), precious metals (PMs), platinum group metals (PGMs), metals of concern (MCs, Hazardous), and scarce elements (SEs) [15].

- Base metals (BMs): Cu, Al, Ni, Sn, Zn, and Fe.
- Precious metals (PMs): Au, Ag, Pd, Pt, Rh, Ir, and Ru.
- Metals of concern (MCs, Hazardous): Hg, Be, In, Pb, Cd, As, and Sb.
- Scarce elements (SEs): Te, Ga, Se, Ta, and Ge.

Manual disassembly is a standard procedure that is usually performed on the scrap before metallurgical processing. It is used to separate the components that are rich in valuable metals from the rest of the scrap. In a first step, pollutants such as LCD panels, capacitors, and highly toxic and harmful materials are separated, so that they can be safely discarded without incurring a severe environmental impact. Furthermore, recyclates, e.g., rough pieces of plastic or copper, are removed selectively [3, 16]. Subsequently, several shredding and multiple-sorting steps take place, which separate the input material into different recyclates such as copper scrap and printed circuit boards as well as pollutants and residues [16]. The general procedure is shown in Fig. 1.

Typical waste fractions that occur during the mechanical treatment are dust or shredder light fractions (SLFs) [16]. The amounts of these waste fractions differ for each specific treatment route. According to Bigum et al., the percentage used for treating high-grade WEEE produces up to 3 kg of filter dust and 32 kg of light fraction (fluff) per ton of high-grade WEEE [18].

Thereby, precious metals can be found in dust streams either in the off-gas or on the surface of other output fractions. This is caused by PMs (precious metals) that are usually widespread and only used in small amounts in complex materials of electronic parts or PCBs, which are broken into small pieces during shredding processes [19].

A detailed analysis of the chemical and mineralogical compositions of WEEE fines originating from a mechanical recycling process of waste printed circuit boards was conducted by Wang et al. [20]. With SEM and EDS analysis of the different-sized fractions, they were able to analyze longish fibers consisting of mainly Al, Si, and Ca and metal particles composed of mainly Al, Cu, and Fe. The amount of metal particles decreased with the increasing particle size [20].

Pyrometallurgical e-waste recycling is mainly carried out in plants using an equipment that was initially developed for the primary extraction or remelting of copper and lead. In a typical smelting process for electronic wastes, the e-wastes are fed together with other nonferrous metal scrap and scraps containing precious metals into melting furnaces or converters (i.e., IsaSmelt or Kaldo). The process usually takes place at temperatures around 1300 °C. Oxygen or enriched air is injected into the furnace for organic content combustion and to melt the load. Thereby, the organic content substitutes parts of the fossil fuels and supplies energy to the system. At the same time, a selective oxidation takes place with the metal impurities present in the feed. These oxidized metal impurities then form the slag phase along with the ceramic materials found in the e-wastes [21].

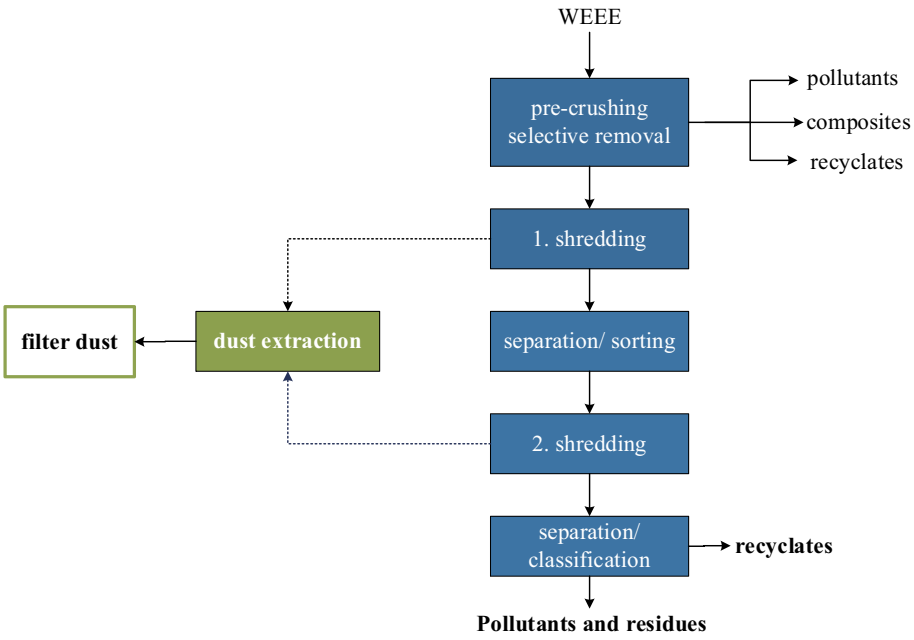

Fig. 1 General mechanical treatment of electronic scrap [16, 17] (Color figure online)

An Innovative Approach for Introducing Powdered WEEE into a Molten Slag Bath

Due to the high content of valuable metals in WEEE powders coupled with a lack of suitable methods for recovering these fractions in the melting process, the IME investigates the introduction concepts of powders into the slag phase. These methods are able to address all of the aforementioned aspects:

- Limitation of input because of the exothermic reaction by organics and oxygen.
- Deviation of slag properties due to incoming impurities.
- Challenges caused by small particle size, which can result in high material losses into the off-gas and the reaction of particles before they enter the reaction zone.

It is therefore important to investigate the influence and the effects of the dusts on the slag phase. Thus, the following aspects are of great importance:

(1) Liquidus temperature.
(2) Viscosity influenced by oxidic and ceramic constituents.
(3) Required oxygen amount for combustion of the entire organic content and selective oxidation (Fe, Al).
(4) Metal agglomeration as droplets and their settling through the slag phase.

Dusts from WEEE conditioning already contain high amounts of carbon that accompany the organics, which have to be oxidized and combusted in order to extract the metals. On the one hand, this can be economical and environmentally beneficial in terms of energy and CO_2 balance when it is able to substitute fossil fuels, but on the other hand, a large amount of energy is released in the smelting process that needs to be dealt with.

Besides the high amount of energy, the high contents of silica and alumina in WEEE dusts are very challenging in terms of slag control and adjustment, once they become part of the process. The general idea behind addressing these issues and the complexity of their nature are shown in detail in Fig. 2. The mixed dusts with fluxes are introduced into the basic slag phase consisting of SiO_2, Al_2O_3, and CaO. The added fluxes have to be chosen according to the introduced amount of Al_2O_3, FeO/Fe_2O_3, and ceramics to ensure feasible process properties due to a possible melting point and viscosity deviation. In the slag, metallic aluminum will be combusted, and the majority of the iron will be oxidized by injecting pure oxygen.

The exothermic reaction of the organic combustion is used as process heat in order to melt the contained metal and ceramic components which are collected in a molten bath. Due to their free Gibbs energy, metals such as copper or nickel and precious metals are supposed to remain in the metal phase, whereas losses of lead and zinc will occur due to their high vapor pressures.

The concept behind an investigation on the metallurgical effects of introducing powdered WEEE in a molten slag bath begins with the characterization of the input material used. Subsequently, the analyzed composition is modeled using the software FactSage™ in order to calculate the addition of slag additives and oxygen. This optimized mixture is tested in preliminary laboratory-scale

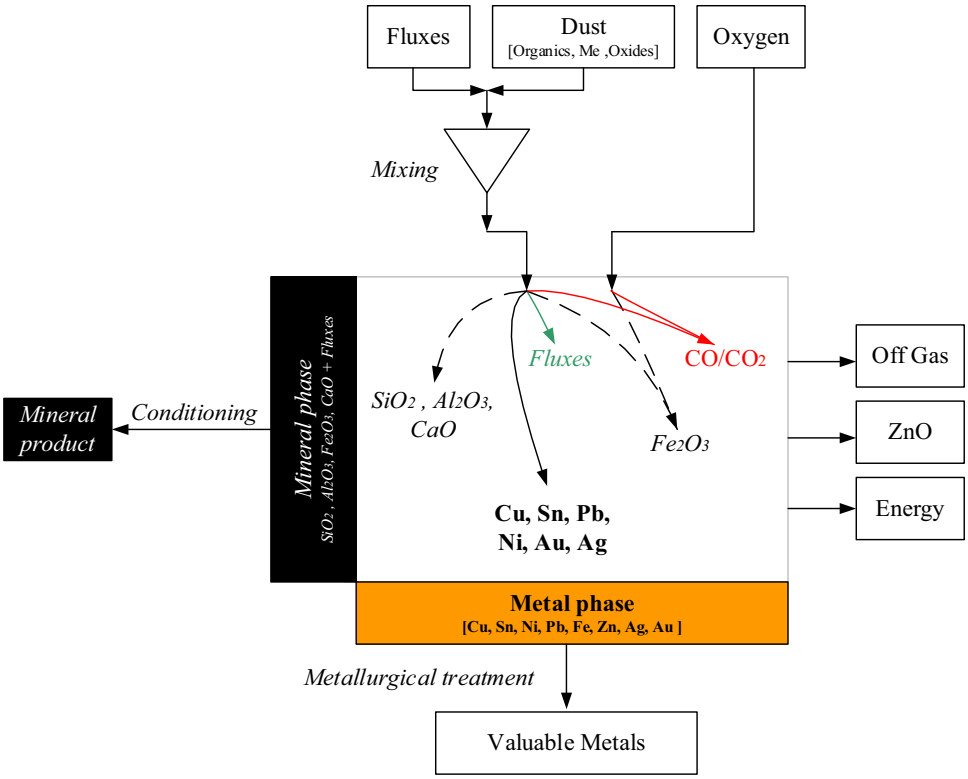

Fig. 2 Process for efficient metal recycling from filter dust (Color figure online)

experiments with input material of 300 g and then expanded to demonstration-scale experiments in a top-blown rotary converter (TBRC) with a melting volume of 500 L.

Material Characterization

Laboratory-Scale Experiments

Microscopic images illustrate the inhomogeneity of the material. Glass fibers from shredded PCBs, metallic particles, and colored particles (most likely plastic) can be identified. A grain-size distribution shows that nearly 50% of the particles are smaller than 50 µm. The detailed average chemical composition is shown in Fig. 3.

The high copper content of 6–10 wt% and the amount of precious metals such as silver (530 ppm) emphasize the recycling potential of the dust. Due to the high contents of Al_2O_3 and SiO_2, a high melting slag phase is generated which needs to be optimized.

Scaled-Up Experiments

Because of the increased material consumption for scaled-up experiments, it is impossible to use the same dusts and powders as in the laboratory experiments. In order to validate the results of the laboratory experiments and to see what kinds of effects the powders and dusts will have on

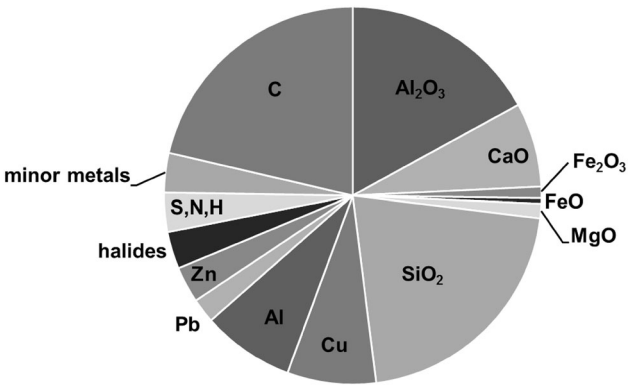

Fig. 3 Average complete chemical composition of filter dust

the slag phase, a material as similar as possible and in sufficient amount was synthetically produced. Therefore, the shredded WEEE scraps of various categories were mixed and grinded to obtain a fine powder comparable to the dusts that were previously used.

Process Modeling

Oxygen Demand

A detailed determination of the oxygen amount required for the combustion of organic contents in WEEE powders

is of great importance for a balanced melting process. On the one hand, the organic contents should be combusted as energy-efficiently as possible. This means that only a few parts of unburned carbon/organics should remain in the off-gas stream, and that, on the other hand, the injected amount of oxygen should determine the reactor's atmosphere.

Due to the high complexity and the heterogeneity of the different PCB categories, fixed oxygen values are impossible. Because of the varying contents of carbon, hydrogen, and easily oxidizing metals such as aluminum, each scrap type requires a different calculation of the oxygen amount required. The calculation of the oxygen required is based on a general plastic composition of PCBs according to Table 1. Based on the measured carbon content, the weight of the organics was calculated. Here 30 wt% C is equivalent to 40–45 wt% of organics. In addition to the organic constituent parts, the oxidation values of aluminum, zinc, as well as parts of iron, lead. and tin were taken into account.

The oxygen value has to be set so that the following assumptions are fulfilled:

(1) The aluminum and zinc are completely oxidized.
(2) The carbon will be completely oxidized to carbon monoxide.
(3) The iron, tin, and lead will be partly oxidized (Comment 5).

All other metals should be collected and recovered in the molten metal phase. Therefore, the oxygen value should not exceed the calculated value, as otherwise, oxidation process of these valuable metals will occur. Furthermore, the oxygen required (if it is assumed that only carbon is present) will be compared to the oxygen required when a general plastic composition is taken into account for the combustion process.

The oxygen amount required for the targeted reaction is around 327 L O_2 per kg of powder and 230 L per kg of dust when only the measured carbon content is taken into account. In case of organics, the oxygen requirement slightly differs due to bound oxygen in the organic compound. The difference between the two assumptions is only 13 L/kg. Hence, for simplification, in the following modeling steps, the organic content will be assumed to be pure carbon.

Phase Equilibrium Modeling

In order to calculate the melting point of the slag, to optimize the melting and the required amount of oxygen for a complete combustion of the plastic content, several modeling procedures were carried out with FactSage™ 7.0. The databases that were used were FToxid (thermodynamic data for pure oxide and oxide solutions), FactPS (pure substances, thermodynamic data for 4776 compounds), and FScopp (copper alloy database). Furthermore, every component was calculated as an initially pure substance.

Slag Melting Temperature

Generally speaking, the liquidus temperature of slags formed by electronic wastes is not predictable and has to be determined on a case by case basis. The basic components of PCBs forming the slag phase are the ceramic constituents SiO_2, Al_2O_3, and earth or alkaline oxides in various compositions [22]. If we only take these elements into account, the general liquidus temperature of e-scraps from type 1–3 varies from 1250 °C up to 1350 °C.

However, in actual recycling processes, e-scraps are always accompanied by components such as casings, resistors, and capacitors which introduce several metals into the process. Alumina and iron have a particularly strong influence on the liquidus temperature because they are easily oxidized and converted into the slag phase. The resulting liquidus temperature strongly deviates from the one previously mentioned with temperatures above 1500 °C, depending mainly on the alumina content in the process. In order to achieve a refractory lining gentle process as well as an efficient separation of metals and nonmetals, an oxidic slag phase with low liquidus temperatures is necessary.

Table 1 General plastic composition of average PCB [22, 23]

Materials	Molecular formula	Molar mass (g/mol)	Part of plastics (wt%)
Polyethylene	$[CH_2]_n$	14	34.02
Polypropylene	$[C_3H_6]_n$	42	16.49
Epoxies	$[C_{15}H_{16}O_2]_n$	228	8.25
Polyvenyl-chloride	$[C_2H_3Cl]_n$	31	8.25
Polyterta-flouroethane	$[C_2F_4]_n$	100	8.25
Polyesters	$[C_{10}H_8O_4]_n$	192	16.49

Slag Modeling for a Reduced Liquidus Temperature

Because of high amounts of alumina, the composition of the slag phase arising from melting filter dust has to be improved in terms of its physical properties. FactSage™ modeling is carried out using a simplified composition which is shown in Table 2.

To calculate the liquidus temperature of the slag, the main oxides (Al_2O_3, SiO_2, MgO, CaO, Fe_2O_2, and FeO) are taken into account. Due to the inhomogeneous material composition, the slag melting point is calculated for the two mixtures (shown by the black point and gray point in the diagram). If the filter dust is processed without optimizing its chemical composition, a liquidus temperature of 1637.4 °C is calculated by thermodynamic assessment for the phase area shown by gray dots (Slag 2). The liquidus temperature for the composition (black dots) is 1490.17 °C (Slag 1) (Fig. 4).

Due to the fact that a slag melting temperature of 1500 °C is unsuitable for a convenient copper recycling process and because of the high formation of solid mineral phases at 1300 °C, it is necessary to optimize the slag. Theoretical influences of different mixtures of SiO_2/CaO on the liquidus temperature are shown in Fig. 5.

A lowering of the melting point is feasible with additions of SiO_2 and CaO down to 1250–1275 °C. An addition in the ratio 0.70 SiO_2 and 0.30 CaO enables a liquidus temperature of 1170 °C but bears the risk of a high viscosity because of the high SiO_2 addition. In order to find a compromise between the melting point and the viscosity, mixtures C and E were chosen for laboratory-scale experiments (pellet mixtures 1 and 2, Table 3).

The liquidus temperature of Slag 2 can be optimized down to 1320 °C. A higher addition also decreases the melting point, but the addition of high amounts of SiO_2 raises questions about the viscosity of the slag generated.

Table 2 Simplified filter dust composition

Compound	Content in wt%	Compound	Content in wt%
C	19.2	Cu	6.83
Al_2O_3	15.3–23.6	Zn	2.79
SiO_2	18.95–21.6	Al	7.10
MgO	1.1–1.7	Sn	0.93
CaO	5.5–6.48	Fe	0.59
Fe_2O_3	0.88	Pb	1.89
FeO	0.42	Ni	0.14
		Au (ppm)	10
		Ag (ppm)	531

CaO can not only be used to lower the temperature, but also serves as a hardener in pelletizing. This optimization was tested in pellet mixtures 7–12. With the addition of Na_2O, a significant decrease of the slag melting temperature down to 1300 °C in the range of 4–10% addition is possible. A higher input of Na_2O leads to the formation of high melting oxides such as $NaAlO_2$ and $NaAlSiO_4$. Despite this theoretical calculation, a mixture with the addition of 15 wt% Na_2O will be tried, in order to test the model. Evaluations about the influences of CaO, Fe_2O_3, and FeO were also conducted.

Modeled Metal Recovery from e-Waste Powders

The theoretical recovery rates in the metal phase for several metals from the filter dust at 1300 °C in relation to the addition of oxygen are shown in Fig. 6. In addition to the maximum use of the combustion enthalpy with the exothermal reaction of carbon and oxygen, a selective oxidation of different target elements was aimed for. Less than 35 L per 100 g of filter dust oxygen addition, copper, nickel, and tin are mainly in the metal phase. A higher amount of oxygen leads to losses of these elements in the slag phase. Aluminum is the first metal to be oxidized after the removal of carbon, which is completely removed with O_2 additions above 0.7 L per 100 g of filter dust, while some carbon is still present in carbides, mainly coupled with iron. Zn and Pb are also present in the metal phase, but are mainly found in the gas phase due to their high vapor pressures at 1300 °C. In the range of 5–25 L, the formation of a face-centered cubic (fcc) solid solution lowers the metal recovery rates of nickel and silver.

The carbon content is completely combusted with an oxygen addition greater than 24 L per 100 g of filter dust. However, based on the results shown in Fig. 6, the theoretical addition of oxygen is defined as 28–30 L of oxygen per 100 g of filter dust (gray area) in order to achieve a satisfactory oxidation of iron (> 92%) and to recover the entire copper amount (> 99%) in the metal phase. Moreover, nearly the entire gold and tin contents can be recovered in the metal phase in this area.

Due to the fact that the slag melting temperature calculated without optimization was too high for a copper recycling process, the slag system needs to be improved by slag additives. When calculating the equilibrium by alternating the addition of oxygen to our system, the results indicated the formation of a gas phase, a liquid metal phase, a solid solution, and different oxide phases depending on the addition of oxygen. The liquid metal phase 1 consisted mainly of copper and was stable up to the addition of up to 42 L of oxygen. The addition of a low amount of oxygen (< 5 L) led to the formation of a second, iron-rich metal phase (liquid 2). The emerging slag phase

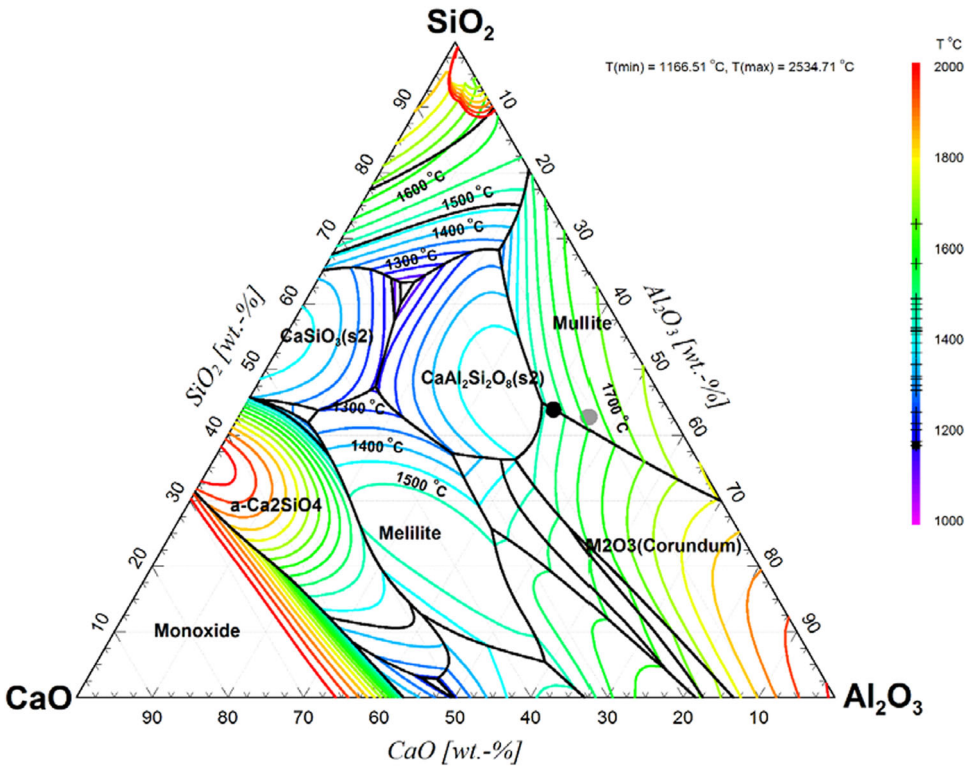

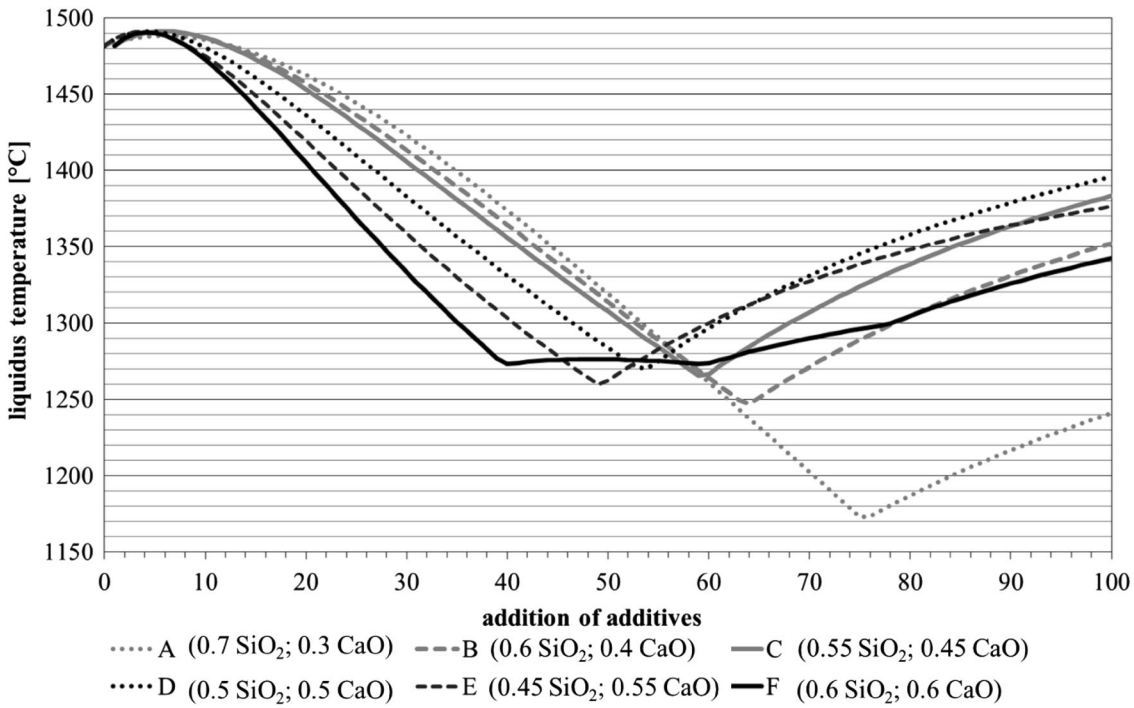

Fig. 4 Ternary phase diagram of the three main oxides with constant values for Fe_2O_3, FeO, and MgO (compare with Table 2) (Color figure online)

Fig. 5 Theoretical influences of different mixtures of SiO_2/CaO on the liquidus temperature

(> 38 L oxygen) mainly consisted of SiO_2, Al_2O_3, CaO, MgO, FeO, and Fe_2O_3. The high amounts of solid oxides, e.g., spinel phase, feldspar, cordierite, and mulite emphasize the need for slag optimization. In maximum, a mass of 60 g of different solid phases arise. With the addition of 10 wt% Na_2O, it is nearly possible to avoid the building of solid mineral phases and to dissolve the oxides in the slag

Table 3 Pellet mixtures for melting experiments

	Slag additives (%)	Binder	Additives	Slag system
Reference experiment	None	None		
1	27.6 CaO; 23.0 SiO_2	molasses	–	1
2	27.0 CaO; 32.4 SiO_2	molasses	–	1
3–5	5.0–15.0 Na_2O	molasses	–	1
6	10.1 CaO; 0.82 Fe_2O_3 0.58 FeO; 6.9 Na_2O	molasses	–	1
7	35.0 CaO; 51.8 SiO_2	molasses	–	2
8	35.0 CaO; 51.8 SiO_2	molasses	10% copper (fine)	2
10	35.0 CaO; 51.8 SiO_2	molasses	10% copper (fine)	2
11	35.0 CaO; 51.8 SiO_2	molasses	10% copper (grains)	2
12	35.0 CaO; 51.8 SiO_2	water	10% copper (grains)	2

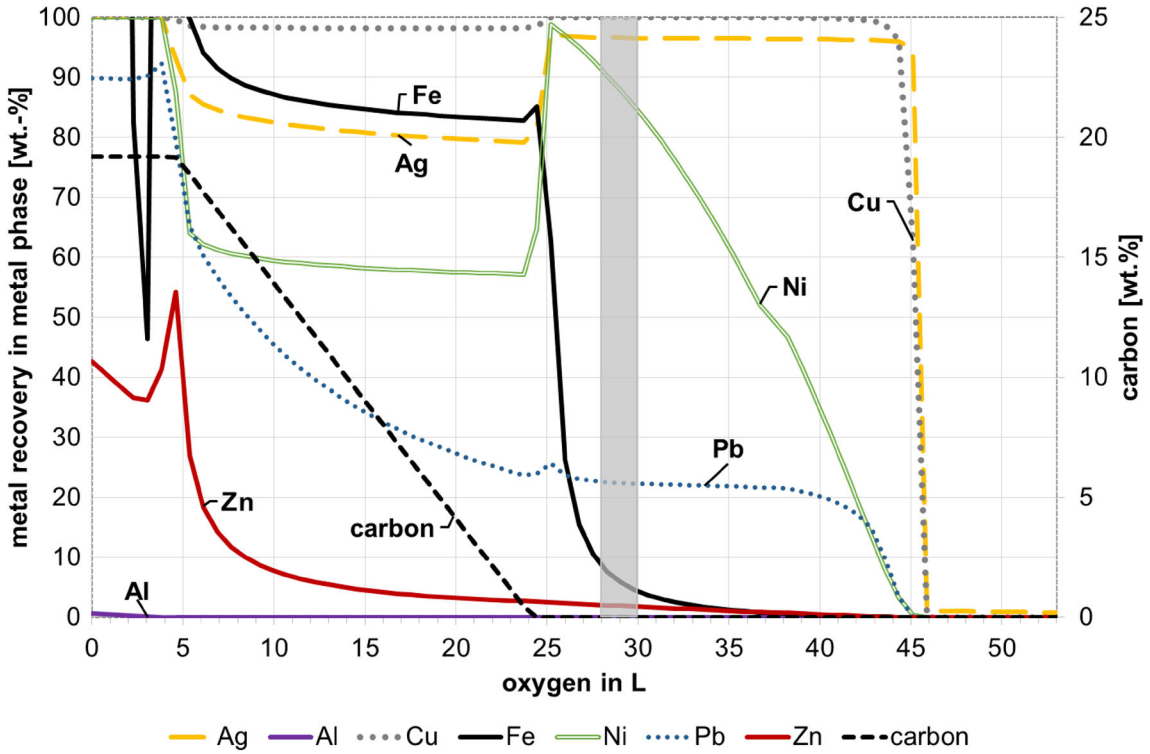

Fig. 6 Metal recovery rates in the liquid phase for several elements at 1300 °C (Color figure online)

phase, and only a small amount of a spinel and carnegieite phase is formed (< 5 g).

To sum up, additives can have positive impacts on the slag phase, decreasing its liquidus temperature and making it much easier (with less time and energy consumption) to reach temperatures above the designated liquidus temperature. This is very important in any pyrometallurgical metal recovery process as increasing the temperature of the slag decreases its viscosity and increases the time that the slag needs to reach its solidification temperature, thus allowing metal droplets to settle and form a homogeneous metal phase. To lower the melting temperature of high melting scrap types like filter dust, the addition of SiO_2/CaO or Na_2O can reduce the melting temperature significantly. A combustion of the entire organic content and a selective oxidation of iron are possible with the defined amount of oxygen.

Experimental Part

Laboratory-Scale Experiments

In order to verify the results from the thermodynamic modeling, the melting behavior of autogenous pellets was tested in an experimental setup as shown in Fig. 9. Pellets

were built up on a pelletizing disk. Different binders, slag compositions, and copper additives were used as listed in Table 3. Pure copper (fine grains) was added to several pellets in order to test and control the exothermic reaction of carbon and oxygen.

Due to the small amounts of filter dust that were prepared (200–300 g), the pellet sizes varied. Most pellets were in the range of between 4 and 10 mm in diameter. Before combustion, the pellets were dried at ambient conditions for 24 h. Water as a binder resulted in an exothermic drying of the pellets, while molasses (water solution with 10 vol% molasses) resulted in a slower drying process.

Kinetic Trials

In order to understand the thermal behavior of agglomerated filter dust and to transfer this to the combustion and melting behavior, laboratory experiments with single pellets were conducted. Here, the weight loss and the temperature inside the core of a single pellet in relation to the time in the furnace were measured and are shown in Fig. 7 for a furnace temperature of 840 °C.

The weight loss for a single pellet (1.5–2 g) was in the range of between 30 and 35%. This decrease started 3 s after placing the pellet in the furnace and continued for up to 90 s. The measurement of the core temperature demonstrated how it took the entire reaction time in the furnace to reach the surrounding furnace temperature. Samples from the core and the shell of the pellet were taken after a defined time inside the furnace. In these samples, the organic carbon was measured in order to obtain information about the reaction progress. High temperatures led to different decomposition steps of the carbon, which also depend on the atmosphere. In these trials, the decreasing carbon content was an indicator of the decomposition and the reaction progress in the pellet. Results of the normalized decrease in carbon in relation to the treatment time are shown in Fig. 8.

Figure 8 demonstrates that the carbon content in the shell decreases faster than that in the core. This shows that the conversion of the pellet starts from the outside and works its way to the core. Higher temperatures lead to a faster decrease in the carbon contents in the core and the shell, because of the acceleration of the mass transport and the reaction progress. The formation of a dark shell can be seen in the cross section of one pellet after 10 s at 800 °C, as shown in Fig. 8.

To sum up, the kinetic experiments with single pellets showed that the reaction between the carbon and the gas phase (starting from the pellet shell to the core) depends on both temperature and time. This behavior which starts while charging the material in a hot furnace has to be taken into account to determine the oxygen requirement. The small plastic particle size in powdered WEEE creates a rapid solid/gas reaction. Because of the unidirectional heating phenomena, the pellet is first heated on the outer layer where gas and plastic particles are directly in contact with one another. The reaction of the entire pellet down to the core depends on the ambient temperature, the pellet diameter, and time. The reaction progress between gas and plastic particles can be described by the increase of carbon

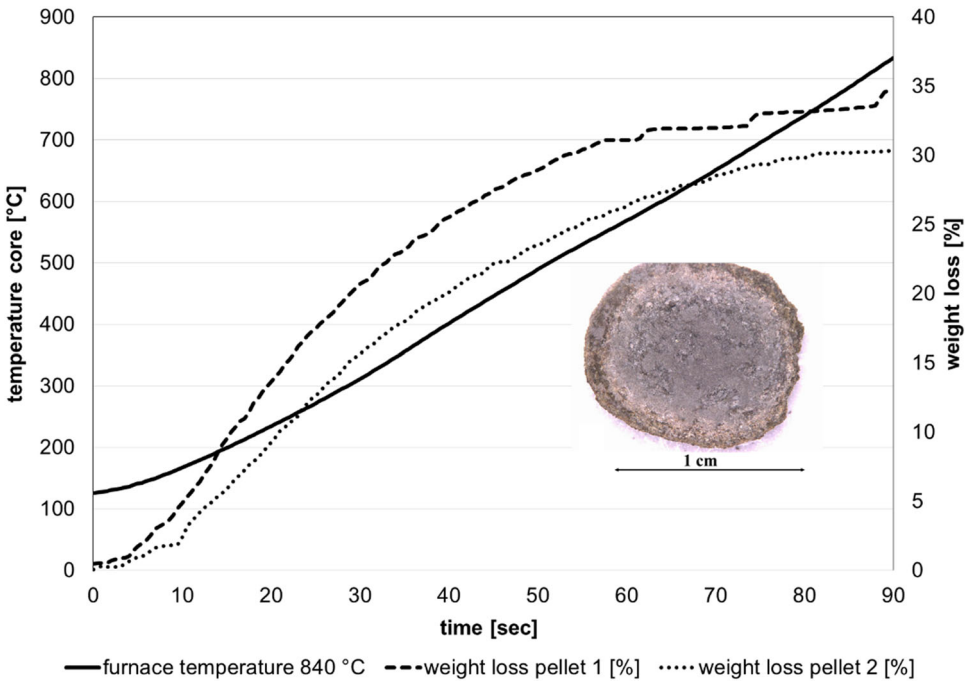

Fig. 7 Weight loss and core temperature of a single pellet (Color figure online)

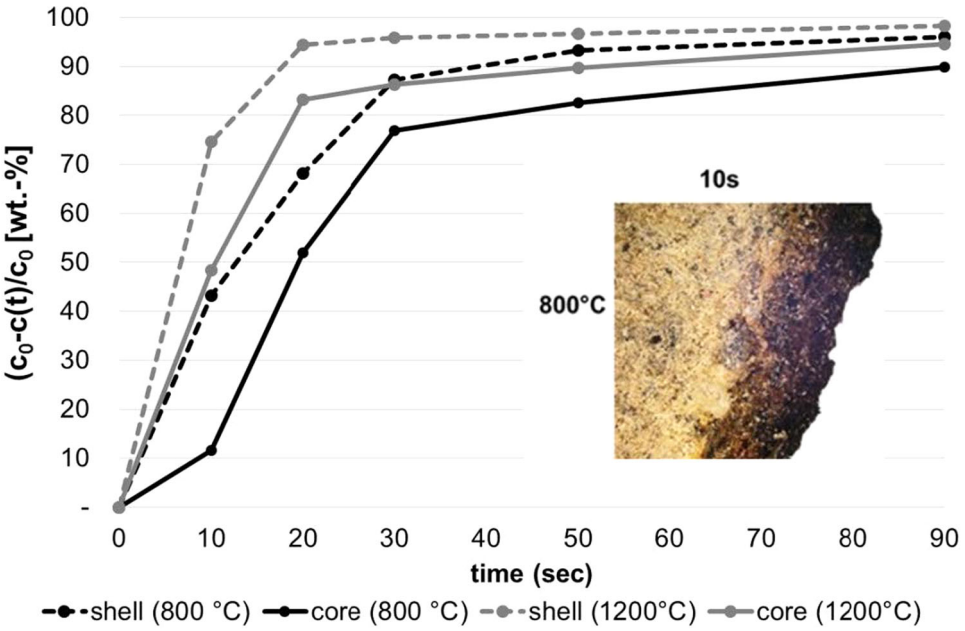

Fig. 8 Normalized losses of carbon in the core and the shell after defined treatment times at different temperatures (Color figure online)

loss. The carbon content decreases with the reaction time, whereby the decrease in the shell is faster compared to the core. Increasing the temperature influences the carbon loss directly to a faster reaction. The reaction time to the core is also shown with the temperature measurement inside the core. These phenomena have a direct influence on the reaction with oxygen and the resulting oxygen amount for the combustion of the organic content. In further research, the mechanism of decomposition and gas–solid reactions will be analyzed in more detail.

Melting Experiments

The laboratory-scale melting experiments were carried out in a resistance furnace. Pellets made of filter dust and the experimental setup can be seen in Fig. 9. Before charging the material, the crucible was heated to 900 °C to ensure that there was sufficient activation energy for the combustion of the organic compounds. A constant oxygen flow ranging between 10 and 15 L/min was injected into the crucible through a ceramic lance. The pellets were charged in batches in order to prevent the lance from becoming blocked. The temperature was measured between the two crucibles, in the off-gas tube and in the crucible before the material was charged. The off-gas composition (CO, CO_2, O_2) was also measured.

The pellets used were stable while they were charged into the crucible and did not show any signs of spalling. After charging, the start of the combustion was visible after 3 s. The resulting liquid phase could only be detected in the parts of the crucible, where the oxygen lance was blowing directly onto the material. After complete combustion, the reaction crucible was taken out of the combustion furnace and placed into another resistance furnace at 1300–1400 °C for one hour to hold the system at the calculated equilibrium conditions. Afterward, the crucible was taken out of the furnace afterward and cooled in ambient air, crushed, and its content manually separated into slag and metal. Samples of slag were analyzed using XRF analysis, while metal samples were analyzed using spark spectrometry.

Results and Discussion for Laboratory-Scale Experiments

To investigate the requirements of the pelletizing step and the optimization of the filter dust composition, combustion experiments with “pure”, nonpelletized filter dust were conducted. In these experiments, it was impossible to achieve a clear separation between the metal and slag phase, and only the formation of small metal droplets on the surface of the material was observed (see Fig. 10). Because of the turbulent off-gas generation (combustion combined with oxygen blow), high material losses > 50% occurred. In summary, more oxygen was required to combust the entire organic fraction compared to that in the theoretical calculation. The actual oxygen amount required for a combustion of the entire organic content was 39–43 L oxygen per 100 g of filter dust.

The melting behavior of the pellets depends strongly on the composed mixture. For some mixtures, a clear separation between metal and slag was achieved. In other cases, high melt viscosity led to an incomplete combustion of the material and to the formation of a solid top layer.

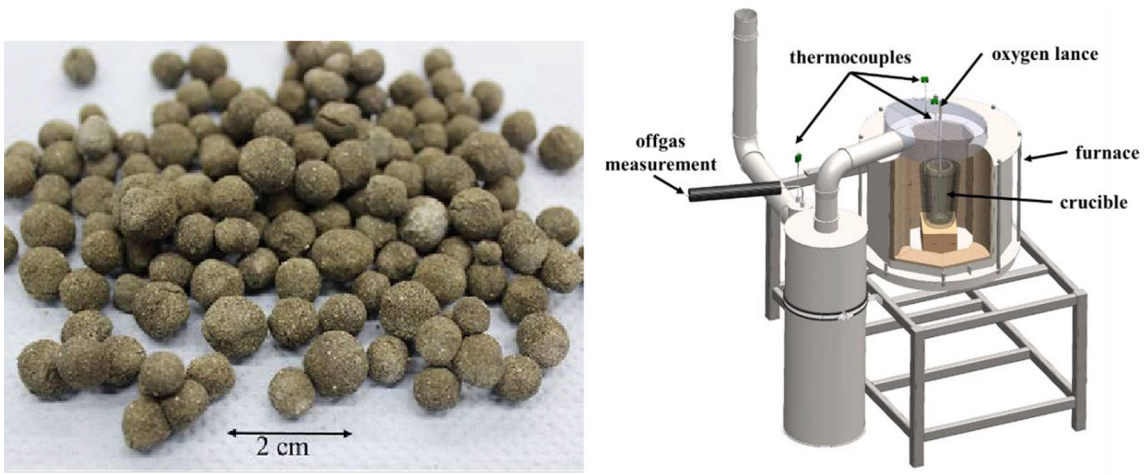

Fig. 9 Pellets made of filter dust (left) and the experimental setup for combustion experiments (right) (Color figure online)

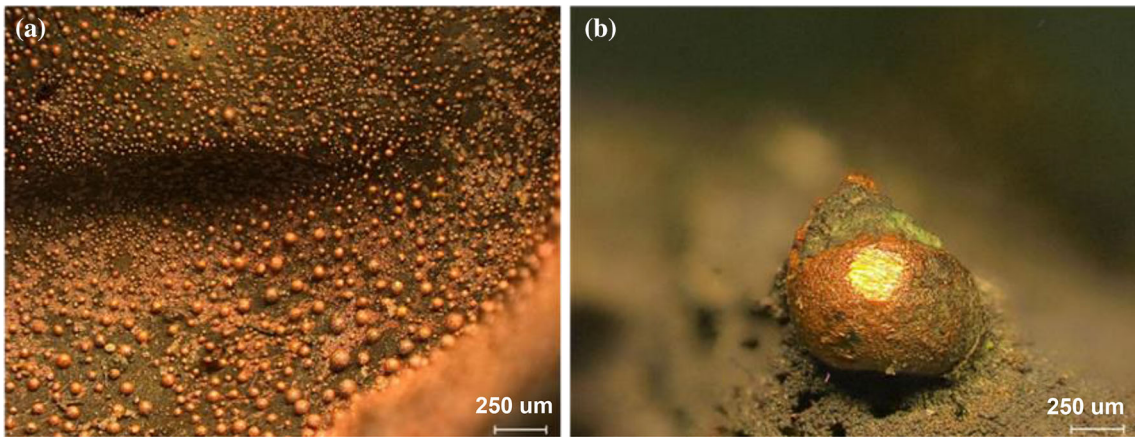

Fig. 10 Metal droplets on the surface after combustion experiments with pure filter dust (Color figure online)

The composition of the metal phase mainly consisted of Cu, Pb, Zn, Sn, and Sb. Other detected elements were precious metals such as silver and gold. The copper amount was between 74 and 96 wt% copper. In experiments with the addition of coper, a higher amount of copper in the metal phase was analyzed. For experiments with the addition of Na_2O up to 8.5 wt% lead was found in the metal phase (mixture 4–6), whereas the lead content in mixture 7–12 was below 1 wt% in the metal phase. Weight loss in the melting experiments was between 30 and 35 wt%, which is in line with the weight loss experiments for single pellets (see "Kinetic trials").

A comparison between the modeled and analyzed metal compositions for selected mixtures 4–6 is shown in Fig. 11. In general, the modeled FactSage^{TM} composition is very much in line with the produced metal phases. For mixture 4, a combination of 10% Na_2O, filter dust and molasses as the binder was investigated experimentally. The calculated melting point of the slag phase was assumed to be around 1300 °C. The oxygen amount required to achieve a clear

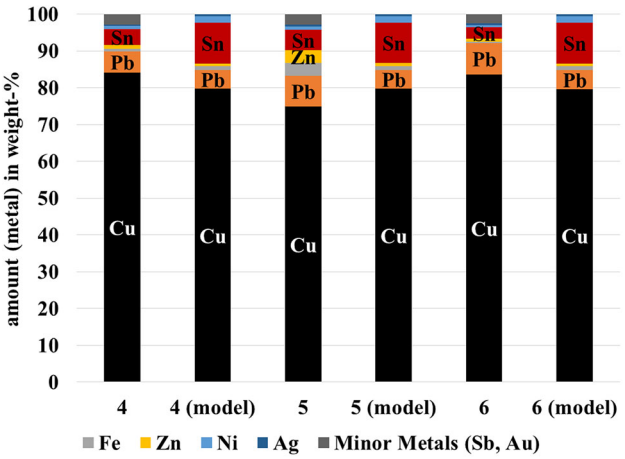

Fig. 11 A comparison between the actual and modeled metal compositions (Color figure online)

separation between metal and slag was 39–42 L per 100 g of filter dust. In experiments with mixture 4, around 6% metal and 50% slag were produced (+ material losses in

off-gas and combustion weight loss). The metal phase contained a higher copper amount (84 wt%) than calculated (79 wt%). Instead, the amount of tin was significantly lower than calculated, which also applies to all metal calculations shown. Due to the fact that the actual oxygen amount was higher than the one calculated, a selective oxidation of a higher amount of metal was possible (see Fig. 6). This supports the fact that the actual iron amount in the metal phase was lower than those calculated in mixtures 4 and 6. The metal phase in experiment 5 contained less copper (74.8% as opposed to 81.2%) than modeled in contrast to the iron amount that was much higher (8.5% as opposed to 4.9%). This can be justified by a segregation of the melt into a copper-rich phase and an iron-rich phase. The equilibrium modeling only predicted segregation in the metal phases for oxygen additions, which was significantly lower in comparison to the actual oxygen addition for mixture 5. This shows that it was not possible to achieve the equilibrium between the metal and the slag phase in the laboratory-scale experiments. The small scale also caused metal losses in the slag phase, which will be optimized in the scale-up experiments (Comment 1).

For precious metals like gold and silver, it was possible to achieve recovery rates that were significantly above 100%. This proved that the input material was rather inhomogeneous and contained more precious metals than those estimated in the calculations. Antimony was found in the produced metal phases, which was not taken into account for the FactSage™ calculation. The model will be extended due to this result in future studies.

A comparison between the actual and the modeled slag compositions for selected experiments is shown in Fig. 12. The chemical slag analysis was normalized to 100 wt%. Only the main and relevant oxides were shown with an individual color. ZnO, PbO, NiO, SnO, and MgO were summarized (rest). Generally speaking, the calculated slag

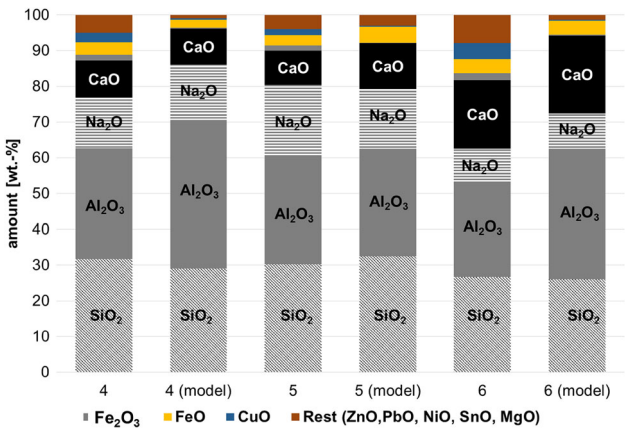

Fig. 12 A comparison between the actual and modeled slag compositions (Color figure online)

composition (FactSage™) showed a good correlation with the analyzed slag composition, especially for the amounts of SiO_2, Na_2O, and CaO. The actual amount of Al_2O_3 was smaller than the ones calculated for all experiments. This observation implies that the content of alumina in the raw material was less than that assumed. In contrast, the contents of iron oxides and copper oxide were higher than those calculated. Analysis showed a copper content of between 1.7 and 4.4 wt% (CuO) in the slag, whereas the modeled amount was < 0.3 wt%. One possible explanation for this is that the material needs a longer time to react and a higher oxygen amount to combust than that assumed. The higher input of oxygen and the small scale of the trials bear the risk of copper oxidation. Higher recoveries of metals such as Pb, Zn, and Sn in the metal phase cannot be achieved because of the small material input and the relatively high oxygen amount. The influences of metal oxides on the slag melting point and its viscosity must therefore be taken into account in further calculations (Comment 3).

To sum up all results from the laboratory-scale experiments, it is absolutely necessary to optimize the high melting filter dust in order to achieve a metal and slag separation. In the small-scale experiment, an addition of 10% Na_2O continuously showed the best results. Calculating the melting point and slag/metal composition with FactSage™ showed a good correlation with the chemical analysis. However, challenges for modeling the melting behavior in laboratory-scale trials with FactSage™ are:

- A significantly higher amount of oxygen due to the kinetics of the reaction of oxygen and carbon in the pellet (see "Kinetic trials") and the unknown oxygen efficiency on the laboratory scale.
- Oversimplification of the actual input material for modeling. Due to this fact, several elements, for example, antimony are not taken into account.
- Due to differences in density and particle size, segregation during storage can occur. The input material is mixed for a defined time before the experiments, but inhomogeneity cannot be ruled out, which has a great influence because of the small scale.
- FactSage™ models are calculations in the equilibrium where kinetics are not taken into account. This influences, for example, the calculations for phase distribution and oxygen requirements.

Scaled-Up Experiments

The laboratory experiments showed the feasibility and potential metal yields by melting WEEE powders. In the next step, the effects of e-waste powders and fines on the slag phase on the small industrial scale (0.5 m^3 melt

volume) were investigated in order to reduce any side effects and to compare the simulated FactSage™ results with the actual melting experiments. Therefore, finely grinded PCBs were injected into a synthetic slag phase at 1300 °C, the starting temperature. Furthermore, it was tested as to whether a foamy slag can be achieved. The general experimental setup is shown in Fig. 13.

The experiments were conducted in a top-blown rotary converter (TBRC) at the IME Institute in Aachen as shown in Fig. 14. The powders and fines were injected into the slag phase near the metal–slag boundary through the main injector. A second injector was optional and not in use for the main process. It can, however, be added in special cases when fluxing is required. The experiment was conducted with an initial molten slag bath formed by a SiO_2, Al_2O_3, and CaO composition, chosen so that the lowest possible liquidus temperature was achieved.

After the slag was completely molten, the powders were injected into the molten slag phase. The mass flow of injected WEEE powders was adjusted according to the calculated energy requirement for an autothermic melting process between 1350 °C and 1450 °C and was based on the calorific value of the previously measured carbon content of 30 wt%. Based on the results of the laboratory trials, the simultaneously injected amount of oxygen was slightly increased to the calculated value of 320 L O_2 per kg powder and later adjusted so that the organics could be completely combusted. After 800 kg of material had been continuously injected into the slag phase and 30 min of holding time had passed at 1450 °C, both, slag and metal phases, were tapped. The produced metal settled at the bottom of the ladle and could be easily separated from the slag after cooling (Fig. 15). Finally, several samples of each phase were taken and analyzed.

Results from the Scaled-Up Experiments

Combustion of Organics Depending on the Oxygen Supply

The combustion of the WEEE powders was executed so that nearly no fumes in the off-gas stream were visible. The gas temperature and composition especially in terms of CO, H_2, and NO_x were continuously measured. In Fig. 16, a characteristic extract of the measured data is shown. Here the actual oxygen amount per kg of powder is shown for two cases: on the one hand, the calculated 320 l oxygen per kg, and on the other hand, the actual oxygen consumption per kg of the injected material. All values are in relation to the actual material mass flow. In addition to the two oxygen consumption rates, the resulting temperature of the off-gas stream is also shown. Primarily, three different intervals can be identified (based on the calculated stoichiometric oxygen requirement):

(I) Low oxygen input: The actual injected oxygen amount is way below the calculated oxygen requirement.
(II) Equal or slightly higher oxygen input than the stoichiometric calculated (incl. 25% O_2 addition).
(III) High oxygen input: The actual injected oxygen amount is well beyond the calculated oxygen requirement.

Interval 1 is exemplary for combustion processes with a lack of oxygen. A first indicator therefore is the increasing

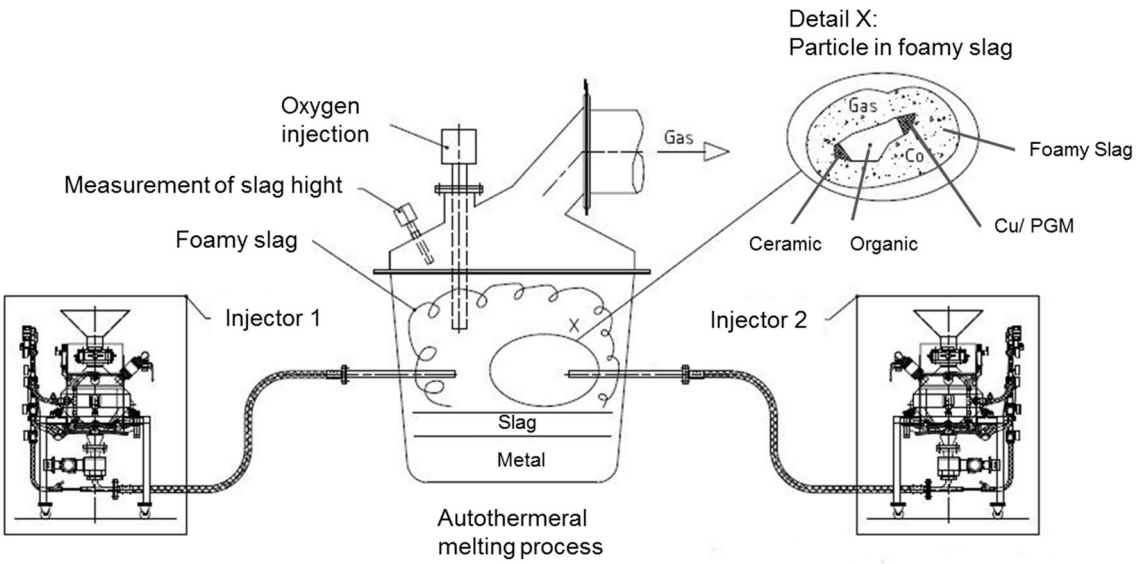

Fig. 13 Schematic process of WEEE powder injection into the slag phase

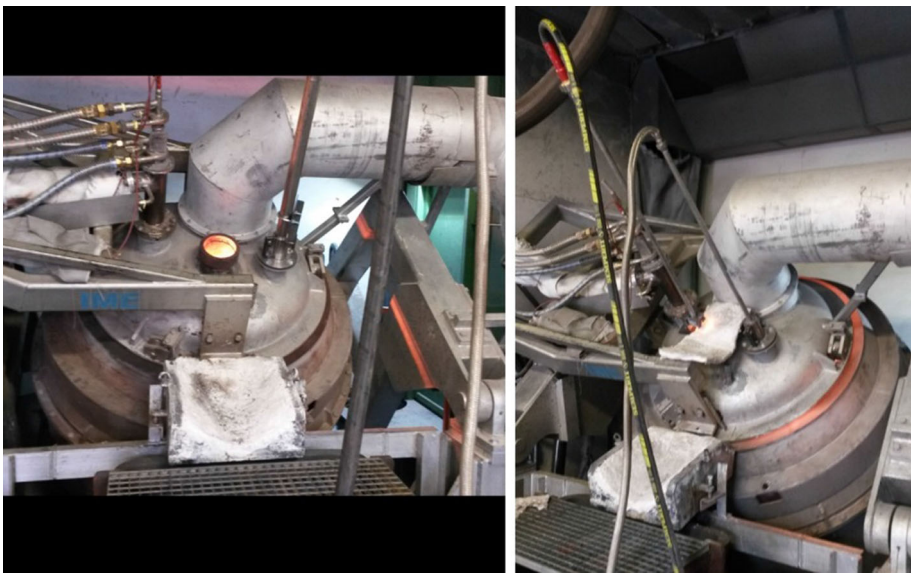

Fig. 14 TBRC with lances for injecting WEEE powders and oxygen (Color figure online)

Fig. 15 Left: Injecting powder into the slag phase; right: Cooled slag and metal block (Color figure online)

off-gas temperature exceeding the material mass flow caused temperature change due to strong post-combustion processes in the off-gas stream. A second and very strong indicator can be seen in Fig. 17. Here the CO, H_2, and NO_x formation is shown for the same time interval as that shown in Fig. 16. The area of phase 1 contains various and very high CO peaks accompanied by visual and distinct H_2 peaks. This results from a lack of sufficient oxygen for combustion. Hence, only CO can be formed. The lack of oxygen is so high that pure H_2 was formed but not post-combusted.

Interval (2b) shows an area of sufficient oxygen requirement, and in the case of interval (2a), even with a small excess of oxygen. These intervals are characterized by a stable temperature and very low CO amounts. In the interval (2b), the oxygen demand nearly equals the 320 L per kg with less oxygen excess than that in (2a). Here a CO formation below 50 ppm can be identified with a few peaks slightly exceeding the 50 ppm value. In the case of H_2 in both intervals (2a) as well as (2b), no relevant peaks are visible. By comparing the two intervals, it can be said that the CO as well as the H_2 amounts in the off-gas are lower with a slightly increased oxygen value.

The same result can be seen in interval 3 where the injected oxygen strongly exceeds the calculated amount. In terms of CO and H_2 formation, no significant change compared to interval (2a) can be seen. Only a strong temperature decrease in the off-gas stream is apparent. The strong decrease results, on the one hand, from a decreased material flow and, on the other hand, from gas excess and reduced post-combustion processes in the off-gas stream.

By comparing all intervals, it is evident that interval 1 is not suitable for the melting process due to the high pollution of the off-gas streams. Moreover, interval 3 is not suitable; even though it shows good off-gas values, the high oxygen content has no significant influence and inevitably leads to an oxidization and loss of valuable metals. The best results were achieved with equal or

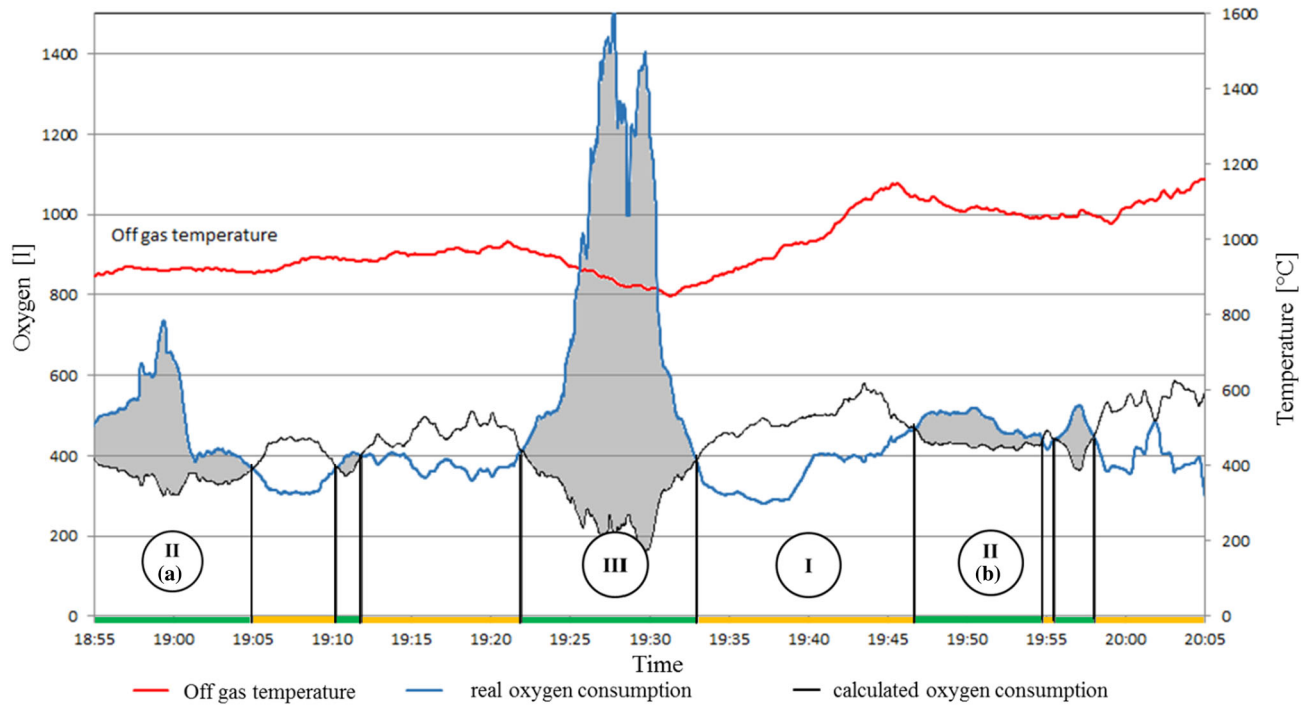

Fig. 16 Comparison of the actual and calculated oxygen consumptions depending on mass flow (Color figure online)

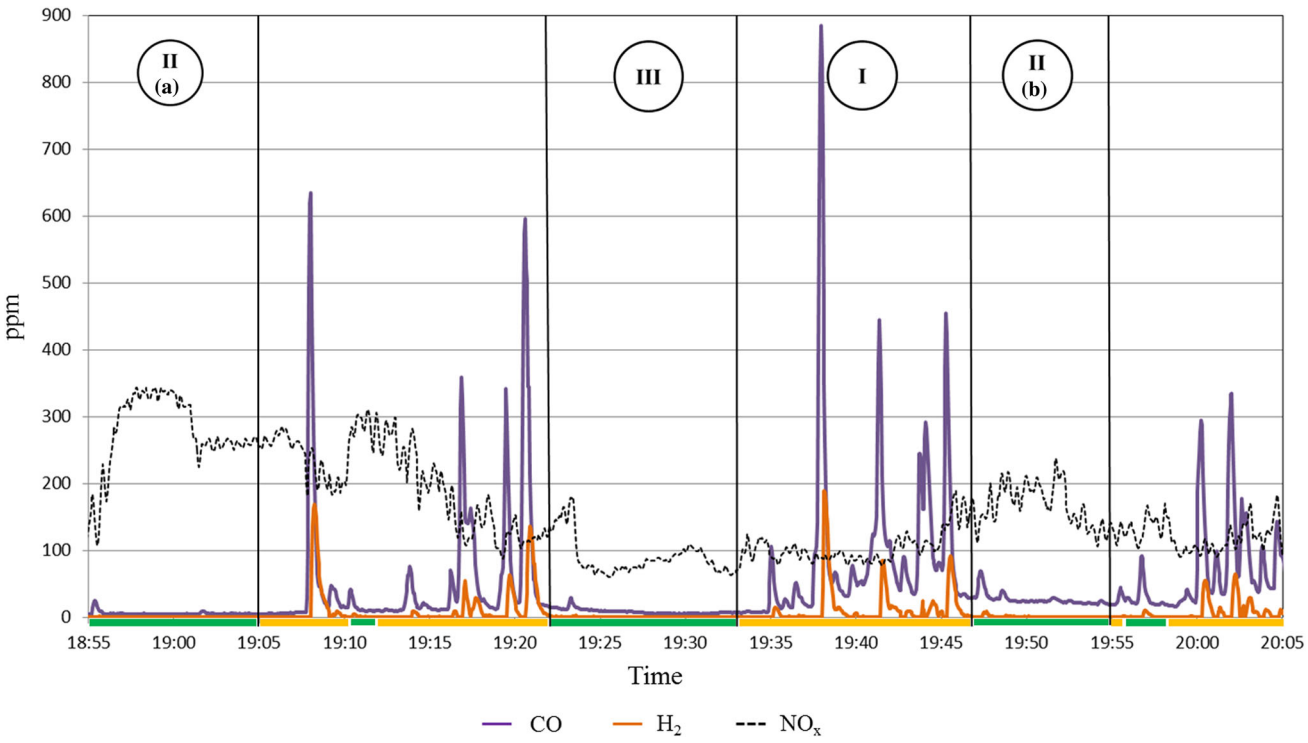

Fig. 17 CO, H_2, and NO_X concentrations in off-gas (Color figure online)

slightly increased oxygen values compared to that for the previously calculated 320 L. Considering only interval 2 process phases, 400 L of oxygen per kg of powder were injected parallel to the material. Compared to the previously calculated value of 320 L per kg of injected material, the actual oxygen requirement appears to be 25% higher

than that assumed. This can be explained by the reaction rate of the oxygen that may not react even though it is injected into the slag because all of the surrounding elements have already been oxidized. The reaction rate under scaled-up conditions seems to be less than that experienced under the laboratory experiments. In terms of NO_x formation, Fig. 17 shows that the average value lies below 300 ppm and, in most cases, even below 200 ppm. Over the entire process, values below 200 ppm were most common. Compared to the values produced by the natural gas burner between 800 and 1100 ppm NO_x depending on operation mode, the values of the autothermal WEEE-powder melting were 75–80% less.

Liquidus Temperature and Viscosity of the Slag Phase

During the entire experiment, the slag was completely molten at temperatures of approximately 1400 °C and showed a low viscosity with no significant changes even though material was continuously injected. Hence, no fluxes were added to the process. It should be mentioned that the evaluation of the slag's viscosity during the process could only be carried out visually and on the basis of experience, due to the high turbulences in the furnace and the slag's foaminess, which exclude all calculation and modeling opportunities. The foaminess of the slag partly resulted from the injected nitrogen and oxygen but mostly from CO/CO_2 bubbles that formed in the slag phase. The foaminess was not as strong as expected. This can be explained by the material flow compared to the reactor size. For a good and strong foaming of the slag, greater carbon-rich material is required in the process. In this particular case, this was impossible due to the already relatively high energy levels at these material input rates.

In terms of liquidus temperature, it appeared that the entire slag phase was completely molten at these temperatures without adding any additives. This experimentally observed completely molten slag phase at approximately 1400–1450 °C in contrast to the calculated liquidus temperatures of both the initial material composition as well as the final slag composition, shown in Table 4, as 1495 and 1514 °C, respectively. Both liquidus temperatures are above the temperature conditions in the furnace.

The great deviation between the measured temperature in the furnace with a molten slag and the theoretically calculated temperature for a complete liquid slag phase with FactSage™ can be explained by an error in temperature measurement even though this was double checked by two independent measurement systems (pyrometer and thermocouple). Another possibility could be an error in FactSage™ calculations due to the exclusion of metallic oxides with a very low percentage of weight although metal oxides such as MgO and TiO_2 were experimentally added to the calculation. However, the liquidus temperature could only be decreased to 1475 °C which is still above the average furnace temperature. The most realistic explanation for the observed effect is a possible high metal content (Cu) in the slag phase during the process, which could not be measured in the cooled slag due to efficient metal settling. A higher Cu content in the slag phase than the measured would lead to significant changes in liquidus temperatures even below 1400 °C and explain the low viscosity and liquidus temperature. To validate this assumption, further tests are necessary with continuous slag sampling.

Table 4 Composition and liquidus temperatures

Wt%	SiO_2	Al_2O_3	CaO	Fe_2O_3	T_{liq} [°C]
Powder	42.6	28.8	18.5	10.1	1495
Slag	38.2	33.8	20.4	7.6	1514

Products and Distribution of Metals

The analysis of the products shows that 277 kg of slag and 96 kg of metal phase are produced with 670 kg of input material. Hence, 56% of the injected material is transformed into metal and slag, whereas 44% is lost to filter dust or the off-gas. The loss within the scaled-up experiments appears to be higher compared to the laboratory trials (30–35% loss) and can be explained by the combustion of the organic content, which has a higher percentage in the injected powder than that in the dust. Furthermore, the discharge of volatile components like Zn is slightly increased at scaled-up experiments. In total, the 44% of material loss is in line with the aforementioned assumption of 40–45 wt% of organics in the material. The detailed analysis of the produced metal and slag phases shows that, on the one hand, the metals of interest were successfully recovered in a metal phase with relatively high recovery rates and that, on the other hand, iron was

Table 5 Metal composition and distribution

Wt%	Cu	Ni	Fe	Pb	Sn	Ag	Mass (kg)
Slag	3.32	0.245	3.92	0.33	1.09	–	277
Metal	92.98	0.994	0.012	0.24	4.88	0.21	96
Distribution coefficient	0.036	0.247	326	1.375	0.223	< 0.001	

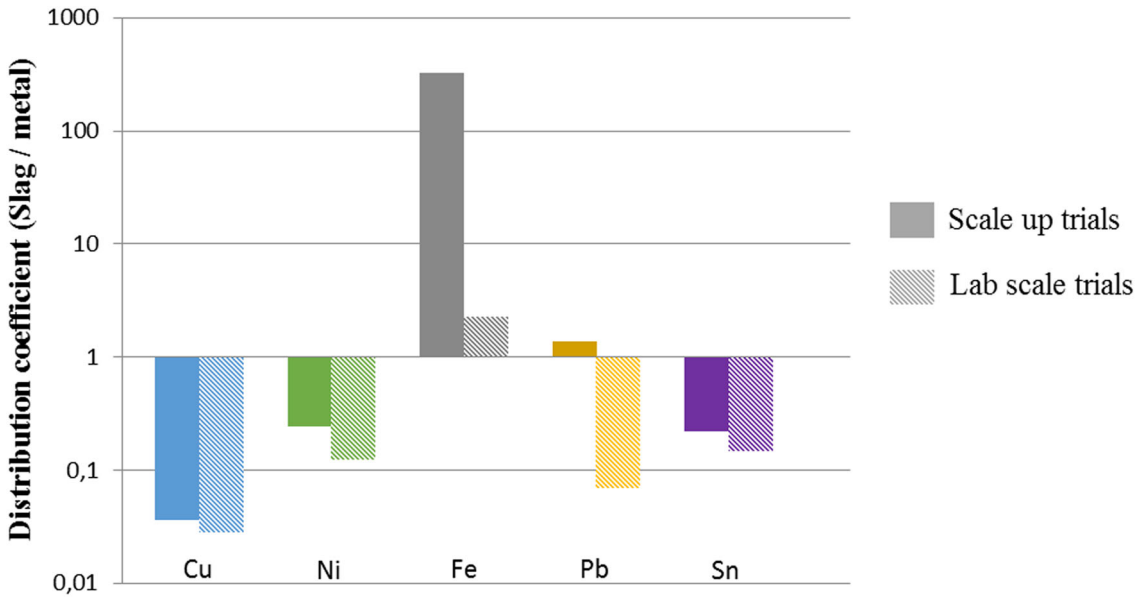

Fig. 18 Distribution coefficients of metals in the laboratory-scale and scaled-up experiments (Color figure online)

selectively oxidized. Table 5 illustrates that nearly 97% of Cu and over 80% of Sn and Ni were recovered. The rest was oxidized and caught in the slag. In terms of iron, nearly 99% was selectively oxidized and transferred to the slag phase.

Conclusion and Open Issues

Laboratory-scale experiments show that it is essentially necessary to optimize high melting scrap types with additives in order to achieve a distinct metal-and-slag separation. To avoid extensive mass losses and to obtain a reaction of the material in the targeted reaction zone, it is necessary to include a pelletizing step or to blow the material in the slag phase. By adding different additives, it is possible to achieve the formation of the slag phase and to avoid the formation of solid mineral phases. The actual oxygen amount required to achieve this separation and to make the entire organic content combustible is approximately 30% higher. One reason for this higher amount required is the amount of oxygen lost to the off-gas system. Furthermore, not only the amount of carbon but also the kinetics for the reaction between oxygen and carbon have to be taken into account, because of the unidirectional heating phenomena from the pellet shell to the core. Studies on the decomposition and gas–solid reactions of carburized pellets will be investigated in future research. Generally speaking, the phase equilibrium modeling agrees with the practical results. Differences occur because the input material is not homogeneous, because of the oversimplified model of the material and because the equilibrium, as modeled in FactSage^{TM}, was not achieved.

The scale up showed that an autothermal melting process with powdered e-waste material is possible without any restriction even when the additives are not included. The experimentally determined oxygen demand validated the results of the lab trails demonstrating that an excess of oxygen is necessary to combust the organics efficiently without strong pollution of the off-gas stream. Under technical conditions, the oxygen excess is slightly decreased to 25% (compared to 30% excess in laboratory experiments), and will be less under even more extreme melting conditions. The injected gases and the CO/CO_2 that were produced, foamed the slag but not as much as was expected. With the increasing material flow, the slag's foaming will also increase due to a greater production of CO/CO_2, which is the main driver for slag's foaming. The results of the melting trial show that 55% of the injected material is recovered in two product phases. Precious metals can be recovered with very high recovery rates of 97% for Cu, and more than 80% for Sn and for Ni. The low Fe content in the metal phase shows that it is possible to selectively oxidize iron and transfer it to the mineral phase.

Figure 18 illustrates a comparison of the metal distribution coefficients between laboratory and scaled-up experiments. Even though the input materials are different, the results show very similar distribution tendencies except for iron and lead. This can be explained by a greater oxidizing atmosphere during the scaled-up experiments and a faster oxygen–material reaction due to the increased reaction surfaces compared to that of the pelletized material. Despite the atmospheric influences on iron and lead,

valuable metals such as copper, nickel, and tin are collected in a metal phase with high recovery rates but with a slightly decreased metal distribution coefficient for the metal phase compared to the laboratory experiments.

The experiments show that it is possible to introduce powdered e-waste fractions and dusts into a molten slag phase. Further investigations should be conducted on gas/solid reactions and the autogenous combination of dusts with other waste fractions. In terms of organic combustion and selective oxidation, the oxygen input has to be optimized and precisely adjusted to the mass flow according to the experimental results. Furthermore, studies on the copper content during melting and its development have to be carried out in order to explain and match the observed effects with the simulation results.

Acknowledgments We offer our special thanks to the Stein Injection Technology GmbH for providing the injection equipment and the knowhow. This project is promoted by the federal Ministry for Economy and Energy according to a decision of the German federal parliament.

References

1. Baldé C et al (2015) The global E-waste monitor—2014. United Nations University
2. Rhamdhani M et al (2014) Metal extraction processes for electronic waste and existing industrial routes: a review and australian perspective. Resources 3(1):152–179
3. Veit H, Bernardes A (2015) Electronic waste: recycling techniques. Springer, Berlin
4. Bartos R et al (2015) Stahlfibel. Verlag Stahleinsen GmbH
5. Wang S et al (2003) Verhalten der Reduktion und Volumenänderung von selbstreduzierenden Pellets mit DSD und Kohle als Reduktionsmittel, 18. Aachener Stahlkolloqium, pp 29–41
6. Kowitwarangkul P (2014) Reduction behavior of self-reducing pellet (SRP) for low height blast furnace. Steel Res Int 85(11):1501–1509
7. Nascimiento RC et al (1999) Kinetics and catastrophic swelling during reduction of iron ore in carbon bearing pellets. Ironmak Steelmak 26(3):182–186
8. Lahiri AK et al (2004) Foaminess of slag: cause and control. In: VII international conference on molten slags fluxes and salts. The South African Institute of Mining and Metallurgy, Johannesburg
9. Liukkonen M et al (2012) A compilation of slag foaming phenomenon research theoretical studies, industrial experiments and modelling. VTT Technology 63
10. Merz M et al (2006) New slag foaming experiences with high-chromium steels. Stahl und Eisen 126(1):49–53
11. Shaw D (1996) Recycling of oily millscale and EAF-baghouse dust by re-injection into an EAF using the carbofer process. Working party on steel, seminar on the processing, utilization and disposal of waste in the steel industry, Ungarn
12. Liebman M (2000) The current status of electric arc furnace dust recycling in North America, in Recycling of metals and engineered materials. Wiley, Hoboken
13. Krüger J et al (1998) Einsatz von sekundären, zink- und bleihaltigen Materialien bei der Sinterröstung im Imperial Smelting Prozess. Rohstofftechnik im Wandel, Aachener Umwelttage der Fakultät für Bergbau, Hüttenwesen und Geowissenschaften
14. Wang R et al (2014) Recycling of non-metallic fractions from waste electrical and electronic equipment (WEEE): a review. Elsevier, Amsterdam
15. Hagelüken C (2006) Improving metal returns and eco-efficiency in electronics recycling—a holistic approach for interface optimization between pre-processing and integrated metals smelting and refining. In: Proceedings of the 2006 IEEE international conference
16. Rotter V et al (2014) Anlagenbilanzierung als Bewertungsinstrument für eine Qualitäts-recycling von Elektroaltgeräten. Recycling und Rohstoffe 7:191–203
17. Martens H (2011) Recycling von Elektro-und Elektronikaltgeräten. In: Recyclingtechnik, pp 273–301
18. Bigum M et al (2012) Metal recovery from high-grade WEEE: a life cycle assessment. J Hazard Mater 207–208:8–14
19. Chancerel P et al (2009) Edelmetallrückgewinnung aus Elektro- und Elektronikaltgeräten durch Aufbereitung. Müll und Abfall 2:78–82
20. Wang F et al (2015) Mineralogical analysis of dust collected from typical recycling line of waste printed circuit boards. Waste Manag 43:434–441
21. Espinosa D et al (2015) Electronic waste: recycling techniques (chapter 8). Springer, Berlin
22. Shuey SA et al (2006) Pyrometallurgical processing of electronic waste. In: SME Annual Meeting
23. Ogunniyi IO et al (2009) Chemical composition and liberation characterization of printed circuit board comminution fines for beneficiation investigations. Waste Manag 29(7):2140–2146